JACS
JOURNAL OF THE AMERICAN CHEMICAL SOCIETY
Article
pubs.acs.org/JACS

NMR Method for Characterizing Microsecond-to-Millisecond Chemical Exchanges Utilizing Differential Multiple-Quantum Relaxation in High Molecular Weight Proteins

Yuki Toyama,[†,‡] Masanori Osawa,[†,§] Mariko Yokogawa,[†,§] and Ichio Shimada*[,†]

[†]Graduate School of Pharmaceutical Sciences, The University of Tokyo, Hongo, Bunkyo-ku, Tokyo 113-0033, Japan
[‡]Japan Biological Informatics Consortium (JBIC), Aomi, Koto-ku, Tokyo 135-0064, Japan

Supporting Information

ABSTRACT: Chemical exchange processes of proteins on the order of microseconds (μs) to milliseconds (ms) play critical roles in biological functions. Developments in methyl-transverse relaxation optimized spectroscopy (methyl-TROSY), which observes the slowly relaxing multiple quantum (MQ) coherences, have enabled the studies of biologically important large proteins. However, the analyses of μs to ms chemical exchange processes based on the methyl-TROSY principle are still challenging, because the interpretation of the chemical exchange contributions to the MQ relaxation profiles is complicated, as significant chemical shift differences occur in both ^{1}H and ^{13}C nuclei. Here, we report a new methyl-based NMR method for characterizing chemical exchanges, utilizing differential MQ relaxation rates and a heteronuclear double resonance pulse technique. The method enables quantitative evaluations of the chemical exchange processes, in which significant chemical shift differences exist in both the ^{1}H and ^{13}C nuclei. The versatility of the method is demonstrated with the application to KirBac1.1, with an apparent molecular mass of 200 kDa.

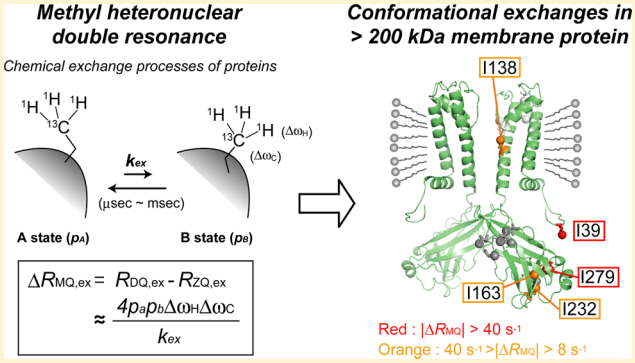

INTRODUCTION

Protein structures are assumed to exist in an equilibrium between multiple conformational substates. Lowly populated conformations in the equilibrium often play critical roles in biological functions.[1,2] Therefore, to reveal the mechanisms of protein functions, it is important to characterize the conformational equilibrium; i.e., the chemical exchange processes of proteins between the highly populated ground state and the lowly populated excited state at an atomic resolution. Solution NMR is a powerful technique for characterizing chemical exchanges on microsecond (μs) to millisecond (ms) time scales,[3] where many biological processes occur.[4,5] A number of sophisticated NMR methods, including ZZ-exchange,[6,7] chemical exchange saturation transfer,[8] Carr−Purcell−Meiboom−Gill (CPMG) relaxation dispersion (RD),[9,10] analysis of dipolar−dipolar/chemical shift anisotropy (CSA) relaxation interference effects,[11] and $R_{1\rho}$ relaxation[12] experiments, have been successfully applied to investigations of functional mechanisms, such as ligand recognitions,[13] catalytic reactions,[14,15] protein folding reactions,[16] and active transport processes.[17]

One of the most critical factors limiting the applications of solution NMR is the molecular weight of the proteins of interest. As the molecular weight of the proteins increases, the stochastic fluctuations of the local magnetic fields accelerate the transverse relaxation of the observed spins, leading to signal broadening and sensitivity loss.[18,19] These difficulties have been overcome by developments in methyl transverse relaxation optimized spectroscopy (methyl-TROSY).[20,21] Methyl-TROSY observes the slowly relaxing ^{1}H−^{13}C multiple quantum (MQ) coherences of selectively ^{1}H, ^{13}C labeled side-chain methyl groups in deuterated backgrounds to achieve optimal resolutions and sensitivities, thus enabling NMR studies of large systems with molecular masses reaching 1 MDa.[22−24] Since many biologically important systems, such as membrane proteins and protein complexes, have molecular masses that are in excess of 100 kDa, the development of methyl TROSY-based NMR methodologies to analyze chemical exchange processes has become increasingly important.[25]

However, the analysis of μs to ms chemical exchange processes based on the methyl-TROSY principle is still challenging, due to the relaxation properties of the MQ coherences, as their relaxation rates are affected by both the ^{1}H and ^{13}C chemical shift differences. Only a few methods, such as the MQ CPMG RD method[26] and MQ relaxation measurements,[27] have been reported so far.

In the MQ CPMG RD method, the most frequently used methyl TROSY-based method, the chemical exchange processes are characterized from the deviations of the apparent

Received: December 11, 2015
Published: January 27, 2016

DOI: 10.1021/jacs.5b12954
J. Am. Chem. Soc. 2016, 138, 2302−2311

MQ relaxation rates ($R_{MQ,eff}$), as a function of the CPMG pulse frequencies. However, the characterizations of the chemical exchange processes are often difficult, particularly when significant differences in both the ^{1}H and ^{13}C chemical shifts exist between exchanging multiple states. In such situations, the $R_{MQ,eff}$ rates may be increased or decreased by the applied CPMG pulses, depending on the relative size of the ^{1}H chemical shift difference to that of ^{13}C, leading to difficulties in extracting chemical exchange contributions.[28] Since ^{1}H chemical shift differences are sensitive to conformational changes of proteins, as represented by the ring-current effects caused by neighboring aromatic rings,[29] a methodology is needed to comprehensively analyze the chemical exchange processes with significant chemical shift differences in both the ^{1}H and ^{13}C nuclei.

The analysis of the differential relaxation rates of MQ coherences is a promising alternative approach for characterizing the chemical exchange processes with significant chemical shift differences in both the ^{1}H and ^{13}C nuclei. The difference in the relaxation rates of double quantum (DQ) and zero quantum (ZQ) coherences, ΔR_{MQ} (= $R_{DQ} - R_{ZQ}$), is highly sensitive to the chemical exchange processes,[30−32] as well as the dipolar and CSA cross correlations, which have been utilized to study bond angles and fast internal motions of proteins.[33−35] Assuming a simple two-state (states A and B) chemical exchange process in a fast exchange regime, the exchange contribution to ΔR_{MQ}, $\Delta R_{MQ,ex}$, can be approximately expressed by eq 1, using the exchange rate, k_{ex}, the populations of the two states, p_A, p_B ($p_A > p_B$), and the ^{1}H and ^{13}C chemical shift differences, $\Delta\omega_H$ and $\Delta\omega_C$.[31,32] The equation for slow to intermediate time scales is also presented in the Supporting Information (eq S7).[36]

$$\Delta R_{MQ,ex} = \frac{4\Delta\omega_H\Delta\omega_C p_A p_B}{k_{ex}} \quad (1)$$

Since, in smaller proteins, the dipolar and CSA contributions to the observed ΔR_{MQ} rates of side-chain $^{13}C^1H_3$ methyl groups are relatively small, the significant increase or decrease of the observed ΔR_{MQ} rates mainly depends on the $\Delta R_{MQ,ex}$ contribution.[27,37] Therefore, the chemical exchange processes can be quantitatively characterized by measuring the ΔR_{MQ} rates. Its successful application for a DNA repair enzyme, AlkB, has recently been reported.[38]

However, as the molecular weight increases, the dipolar and CSA contributions increase and contribute to the ΔR_{MQ}, making it difficult to quantify the $\Delta R_{MQ,ex}$ rates from the ΔR_{MQ}. From calculations using the typical interatomic distances in proteins and the reported CSA values,[39] the dipolar and CSA contributions to the observed ΔR_{MQ} rates are estimated to be about 15 s^{-1} with τ_c = 80 ns (corresponding approximately to a molecular mass of 200 kDa) .[37,40,41] Considering that the $\Delta R_{MQ,ex}$ rates are usually on the order of 10 s^{-1}, it is difficult to evaluate the $\Delta R_{MQ,ex}$ rates from the observed ΔR_{MQ} rates in high molecular weight proteins. Thus, a strategy to experimentally determine the $\Delta R_{MQ,ex}$ rates is needed.

Here, we present a novel NMR method, methyl heteronuclear double resonance method (methyl-HDR), to measure the $\Delta R_{MQ,ex}$ rates of side-chain methyl groups in high molecular weight proteins. Since heteronuclear double resonance (HDR) pulses effectively quench the $\Delta R_{MQ,ex}$ contribution in the ΔR_{MQ}, the $\Delta R_{MQ,ex}$ contribution can be extracted by the difference between the observed ΔR_{MQ} value in the presence of HDR and that in the absence of HDR. By measuring the $\Delta R_{MQ,ex}$ rates, the methyl-HDR method enables the sensitive detections and quantitative evaluations of chemical exchanges with both the ^{1}H and ^{13}C chemical shift differences. The versatility of the method is demonstrated with applications involving maltose binding protein (MBP), the FF domain of HYPA/FBP11, and the membrane protein KirBac1.1, which has a molecular mass of over 200 kDa in detergent micelles.

RESULTS

New Experiment for Evaluating the $\Delta R_{MQ,ex}$ Rates, the Methyl-HDR Method. We present a novel NMR method to measure the $\Delta R_{MQ,ex}$ rates of side-chain methyl groups in larger systems, the methyl-HDR method. The methyl-HDR method exploits the fact that the $\Delta R_{MQ,ex}$ contribution can be selectively quenched by applying spin lock radio frequency (RF) fields sufficiently faster in field strength than the chemical exchange processes. Thus, we can obtain the $\Delta R_{MQ,ex}$ rates as the difference of the ΔR_{MQ} rates measured in the presence and absence of the spin-lock field. To quench the $\Delta R_{MQ,ex}$ contribution, we utilized an HDR pulse technique. HDR is a combination of composite pulse trains simultaneously applied to both of the scalar-coupled nuclei (^{1}H and ^{13}C in this study) to achieve synchronous nutation of magnetization.[42−44] During the HDR irradiation, the MQ coherences are highly conserved, enabling the quantitative measurement of the MQ cross relaxation rates.[45] The method can be applied to selectively ^{1}H, ^{13}C labeled side-chain methyl groups in ^{12}C/^{2}H backgrounds conventionally used for methyl-TROSY applications.[46]

Figure 1 shows the pulse sequences of the methyl-HDR experiments, based on the heteronuclear MQ coherence (HMQC) scheme. The experiments are based on the measurements of the cross relaxation rates between the $2C_xH_x$ and $2C_yH_y$ coherences as originally proposed by Kloiber and Konrat.[32] The initial coherences and the observed coherences during the mixing period T_{relax} can be selected by changing the phases, φ_1, φ_2 and φ_4. During the mixing period and the subsequent evolution period, the coherence of interest is of the multiple-quantum variety, which slowly relaxes due to the methyl-TROSY effect. The methyl-HDR experiments based on the heteronuclear ZQ coherence (HZQC) scheme are also presented, in the Supporting Information (Figure S1). In applications to higher molecular weight proteins, where the resolution is critical, the HZQC scheme can improve the resolution in the indirect dimension with only slight decreases in the sensitivity.[27,37]

First, the ΔR_{MQ} rates in the absence of the spin lock field, $\Delta R_{MQ,ref}$, are measured (Figure 1a, Figure S1a). The $2C_xH_x$ coherence is created at the beginning of T_{relax}, and the $2C_xH_x$ (= s_1) and $2C_yH_y$ (= s_2) coherences are observed after T_{relax}. $\Delta R_{MQ,ref}$ (= $R_{DQ} - R_{ZQ}$) can be calculated from the time-dependent evolution of the s_2/s_1 ratio (eq 2).[32] The obtained $\Delta R_{MQ,ref}$ rates correspond to the sum of the dipolar contribution, $\Delta R_{MQ,DD}$, the CSA contribution, $\Delta R_{MQ,CSA}$, and $\Delta R_{MQ,ex}$ (eq 3).

$$\frac{s_2}{s_1} = \frac{\exp(-R_{ZQ}T) - \exp(-R_{DQ}T)}{\exp(-R_{ZQ}T) + \exp(-R_{DQ}T)} = \tanh\left(\frac{\Delta R_{MQ,ref}T_{relax}}{2}\right) \quad (2)$$

DOI: 10.1021/jacs.5b12954
J. Am. Chem. Soc. 2016, 138, 2302−2311

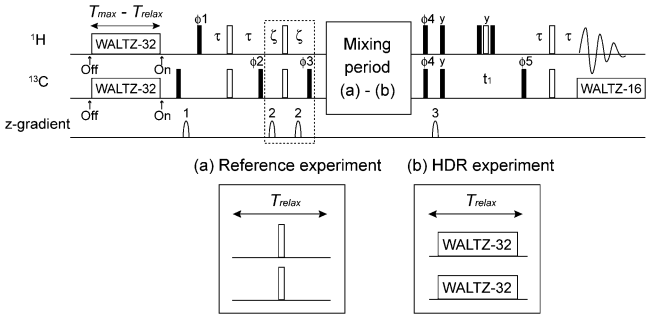

Figure 1. Pulse scheme of the methyl-HDR experiment. Filled and open rectangles represent 90 deg and 180 deg pulses, respectively. Pulse phases are along the x axis, unless otherwise mentioned. The delay τ is set to $1/(4J_{CH})$ and the delay ξ is set to $1/(8J_{CH})$. ^{13}C decoupling during acquisition is achieved with a 3.3−3.6 kHz WALTZ-16 field.[47] The sequence (a) is used during the mixing period (T_{relax}) in the measurement of the $\Delta R_{MQ,ref}$ rates, and WALTZ-32 blocks (b) are used in the measurement of the $\Delta R_{MQ,HDR}$ rates. The WALTZ-32 blocks ($T_{max} - T_{relax}$, where T_{max} denotes the maximum T_{relax} used) are applied at the start of the sequence for heat compensation. The carrier frequencies are set to 5000 ppm for ^{1}H and 25 000 ppm for ^{13}C at the points labeled "Off", and are moved to the methyl regions at the point labeled "On". When cryogenically cooled probes are used, the off-resonance frequencies described above would be rather ineffective as they fall outside of the range where the RF is effectively transmitted to the sample. In such cases, using a smaller frequency difference, eliminiating phase modulation, and placing the element at the end of the FID would probably be preferable.[48] The purge element in the dashed box is employed to eliminate the fast relaxing elements and suppress the artifacts.[26] During the use of this element, the fast relaxing elements ($\Sigma 2C_xH_{x,i}\{|\alpha\alpha\rangle\langle\alpha\alpha| + |\beta\beta\rangle\langle\beta\beta|\}$) evolve due to ^{1}H−^{13}C scalar coupling, and are subsequently eliminated by the application of the $\varphi 3$ pulse and its phase cycle. The element can be eliminated with high molecular weight proteins. To generate the $2C_xH_x$ coherence at the beginning of the mixing period, $\varphi 1 = x$, $\varphi 2 = (y, -y)$, $\varphi 3 = (x, x, -x, -x)$, $\varphi 5 = y$ and rec = $(x, -x)$, while $\varphi 1 = y$, $\varphi 2 = (-x, x)$, $\varphi 3 = (y, y, -y, -y)$, $\varphi 5 = y$, and rec = $(-x, x)$ to generate the $2C_yH_y$ coherence. To detect the $2C_xH_x$ coherence, $\varphi 4 = (4(y), 4(-y))$, while $\varphi 4 = (4(x), 4(-x))$ to detect the $2C_yH_y$ coherence. Quadrature detection is achieved via states-TPPI of phase $\varphi 5$.[49] Gradient strengths (G/cm) are g1 = (15 G/cm, 1 ms); g2 = (−5.0 G/cm, 0.3 ms); g3 = (50 G/cm, 1 ms).

$$\Delta R_{MQ,ref} = \Delta R_{MQ,DD} + \Delta R_{MQ,CSA} + \Delta R_{MQ,ex} \quad (3)$$

Second, the ΔR_{MQ} rates with the HDR spin lock pulses, $\Delta R_{MQ,HDR}$, are measured (Figure 1b, Figure S1b). During the mixing period T_{relax}, the WALTZ-32 HDR scheme is applied for its favorable relaxation properties, regarding the effective auto- and cross-relaxation rates.[45] To compensate for the different effective autorelaxation rates of the $2C_xH_x$ and $2C_yH_y$ coherences under the HDR conditions, the symmetrical reconversion scheme is adopted.[45,50] While the selection of the $2C_xH_x$ coherences at the beginning of T_{relax} provides the $2C_xH_x$ (= s_1) and $2C_yH_y$ (= s_2) coherences after T_{relax}, the selection of the $2C_yH_y$ coherences at the beginning of T_{relax} provides the $2C_xH_x$ (= s_3) and $2C_yH_y$ (= s_4) coherences after T_{relax}. The $\Delta R_{MQ,HDR}$ rates are measured from the time-dependent evolution of the averaged intensity ratio obtained from these four relaxation pathways (eq 4). The difference in the coefficient with the reference experiment by a factor of 2 is derived from the averaging effects of the RF fields.[45] The obtained $\Delta R_{MQ,HDR}$ rates approximately correspond to the sum of the $\Delta R_{MQ,DD}$ and $\Delta R_{MQ,CSA}$, when sufficiently strong HDR pulses are used (eq 5).

$$\sqrt{\frac{s_2 s_3}{s_1 s_4}} = \tanh\left(\frac{\Delta R_{MQ,HDR} T_{relax}}{4}\right) \quad (4)$$

$$\Delta R_{MQ,HDR} \approx \Delta R_{MQ,DD} + \Delta R_{MQ,CSA} \quad (5)$$

Finally, the $\Delta R_{MQ,ex}$ rates can be obtained by subtracting the $\Delta R_{MQ,HDR}$ rates from the $\Delta R_{MQ,ref}$ rates (eq 6).

$$\Delta R_{MQ,ex} \approx \Delta R_{MQ,ref} - \Delta R_{MQ,HDR} \quad (6)$$

The conservations of the methyl-TROSY components are considered in the Supporting Information (Supporting Results 3, Figures S9, S10 and S11).

Even in the cases of proteins with molecular masses of 200 kDa, the dipolar and CSA contributions to the observed ΔR_{MQ} rates are estimated to be about 15 s^{-1}, and are comparable to the values of the $\Delta R_{MQ,ex}$ rates (typically on the order of 10^1 s^{-1}).[32,36] The $\Delta R_{MQ,ex}$ rates are still expected to make large contributions to the $\Delta R_{MQ,ref}$ rates and can be evaluated with high accuracy in higher molecular weight proteins.

The HDR RF field strength of 10 kHz was used, unless otherwise mentioned, for quenching the $\Delta R_{MQ,ex}$ contributions. On the basis of our calculations of homogeneous master equations[51] modified to include chemical exchange processes, the HDR RF field strength of 10 kHz should quench over 95% of the $\Delta R_{MQ,ex}$ contributions when $k_{ex} < 3000$ s^{-1}, and over 85% of the $\Delta R_{MQ,ex}$ contributions when $k_{ex} < 10\,000$ s^{-1}, suggesting that the exchange processes on the order of 10^2−10^4 s^{-1} can be analyzed with acceptable accuracy (Supporting Results 1, Figures S2 and S3). Since the HDR field strength of 10 kHz greatly exceeds the ^{1}H−^{13}C scalar coupling constant (∼130 Hz) and the range of the offsets used in our study (<±1000 Hz), the scalar coupling hardly affects the preservation of the MQ coherence when we use the WALTZ-32 scheme, which was previously reported to be less tolerant of large scalar coupling constants than other composite pulse schemes.[42]

It should also be noted that the off-resonance effects of the HDR RF pulses are moderate under these conditions. Although HDR pulses are very robust in preserving MQ coherences,[42] they are susceptible to off-resonance effects. Therefore, it is recommended to irradiate the HDR pulses on-resonance for both of the coupling nuclei in order to precisely measure the relaxation rates under HDR conditions.[44] However, it is usually difficult to perform a complete set of experiments in which all of the signals are analyzed separately under on-resonance conditions, due to limited experimental time and protein stabilities. With this in mind, we experimentally evaluated the off-resonance effects under HDR conditions, to investigate the possibility of simultaneously measuring the $\Delta R_{MQ,HDR}$ rates of all resonances with a single carrier frequency (Supporting Results 2, Figure S4). When we used the HDR RF field strength of 10 kHz, the systematic errors of the $\Delta R_{MQ,HDR}$ rates ranged from −8% to 11% at the offsets of ±200 Hz, − 17% to 36% at the offsets of ±400 Hz, and −39% to 44% at the offsets of ±800 Hz, as compared with the $\Delta R_{MQ,HDR}$ rates measured under the on-resonance conditions. In practice, the chemical shifts of specific methyl species fall within the range of 0.56 ppm in the ^{1}H dimension and 3.2 ppm in the ^{13}C dimension, as estimated from the standard deviation of chemical shifts in the BMRB database (http://www.bmrb.wisc.edu/), corresponding to 340 Hz in the ^{1}H dimension and 480 Hz in the ^{13}C dimension, assuming a static field strength of 14.1 T (600 MHz ^{1}H frequency). Under these conditions, the systematic errors

DOI: 10.1021/jacs.5b12954
J. Am. Chem. Soc. 2016, 138, 2302−2311

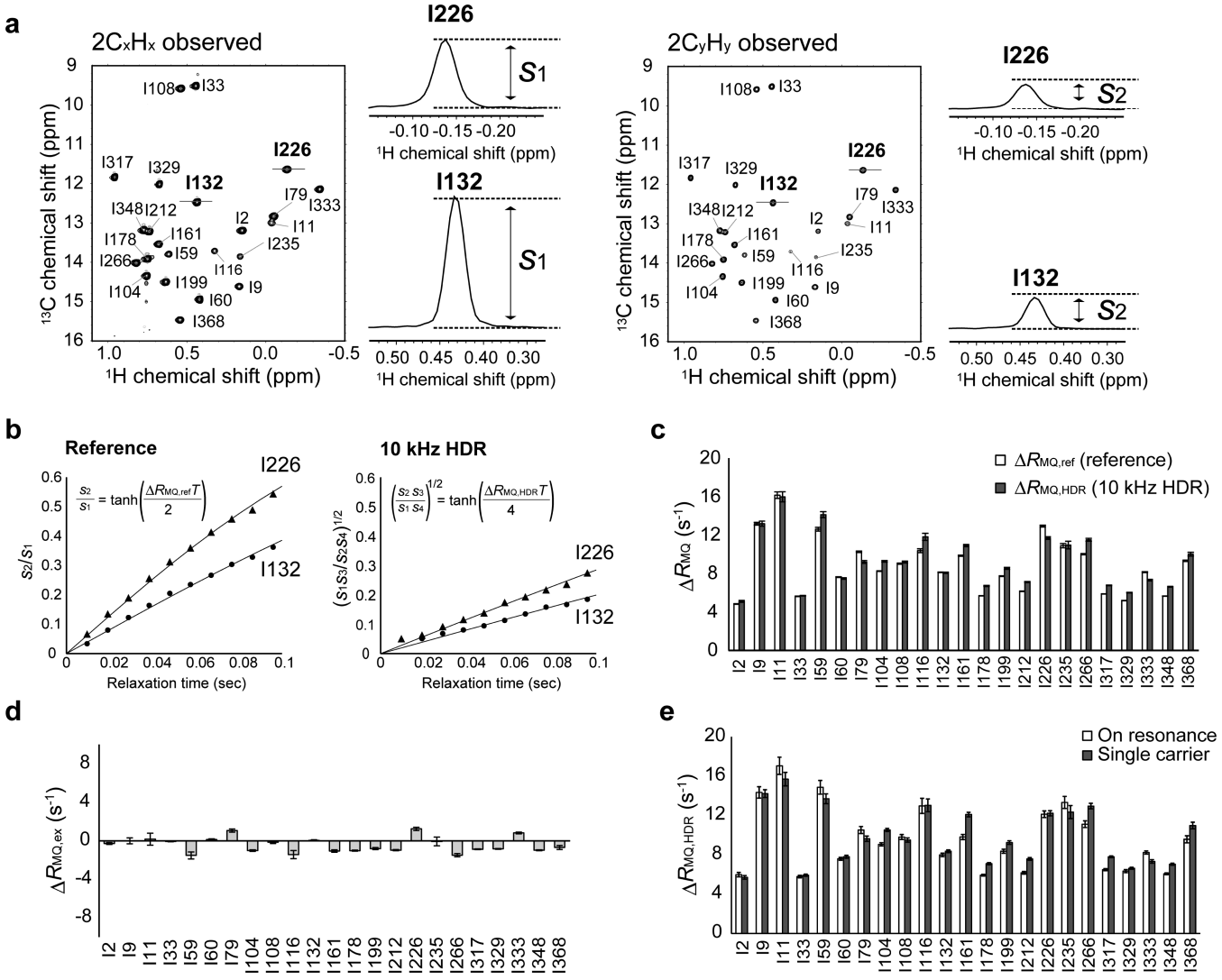

Figure 2. Methyl-HDR results of {u-^{2}H, Ileδ1-[^{13}CH$_3$]} MBP (a) Methyl-HDR spectra of {u-^{2}H, Ileδ1-[^{13}CH$_3$]} MBP observing the $2C_xH_x$ (= s_1, left) and $2C_yH_y$ coherences (= s_2, right) under the initial coherence of the $2C_xH_x$ for measuring the $\Delta R_{MQ,ref}$ rates. The relaxation delay T_{relax} was set to 57.6 ms. The 1D cross sections of Ile132 and Ile226 are shown. (b) Plot of the intensity ratios s_2/s_1 in the reference experiment and $(s_2s_3/s_1s_4)^{1/2}$ in the HDR experiment (eqs 2, 4) against the relaxation period T_{relax} of Ile132 and Ile226. The $\Delta R_{MQ,ref}$ and $\Delta R_{MQ,HDR}$ rates were obtained by fitting the intensity ratios to the theoretical functions. The relaxation delay was varied from 9.6 to 96.0 ms in both the reference and HDR experiments. The fitted curves are shown as solid lines. (c) Plot of the $\Delta R_{MQ,ref}$ rates (white) and the $\Delta R_{MQ,HDR}$ rates (gray) of each Ile methyl group in MBP. (d) Plot of the $\Delta R_{MQ,ex}$ rates of each Ile methyl group in MBP. The $\Delta R_{MQ,ex}$ rates were calculated by subtracting the $\Delta R_{MQ,HDR}$ rates from the $\Delta R_{MQ,ref}$ rates. (e) The $\Delta R_{MQ,HDR}$ rates measured under on-resonance conditions are shown as white bars, and those measured with a single carrier frequency are shown as gray bars. In the experiment with a single carrier frequency, the carrier frequency was set on-resonance to Ile132 (^{1}H chemical shift 0.42 ppm, ^{13}C chemical shift 12.5 ppm). Under these conditions, the Ile methyl signals are distributed across −390 to +260 Hz in the ^{1}H dimension and −370 to +370 Hz in the ^{13}C dimension. The HDR RF field strength was set to 10 kHz and the total relaxation time was set to 48 ms. In all experiments, the measurements were performed at a static magnetic field strength of 11.7 T (500 MHz ^{1}H frequency) using a cryogenic probehead.

are estimated to be smaller than 11%. These results strongly support the proposal that the $\Delta R_{MQ,HDR}$ rates from specific methyl species can be measured with a single carrier frequency and the expected errors are tolerable. However, when some signals show significantly large upfield or downfield shifts, or when samples with various species of labeled methyl groups (e.g., Ile, Leu, and Val) are to be analyzed, it is desirable to measure the $\Delta R_{MQ,HDR}$ rates separately with several carrier frequencies.

Although the RF field strength of 10 kHz apparently exceeds the recommended specification of NMR probes, such strong spin lock fields can be generated by the contemporary cryogenic probes that have been optimized with regard to power management.[52,53] Stronger RF field strengths would achieve complete quenching of the $\Delta R_{MQ,ex}$ contributions and suppress the off-resonance effects. Practically, the maximum available RF field strengths vary among probes, and NMR vendors should be consulted before applying the HDR pulses.

Validations of the Methyl-HDR Method in High Molecular Weight Systems. To validate that the $\Delta R_{MQ,ex}$ values could be correctly evaluated and that sufficient sensitivity could be achieved with high weight molecular proteins, we applied the method to the MBP/β-cyclodextrin complex (molecular mass of 42 kDa). Since significant chemical exchange processes reportedly were absent in the majority of the side-chain methyl groups of MBP,[54] we used MBP as a

DOI: 10.1021/jacs.5b12954
J. Am. Chem. Soc. 2016, 138, 2302−2311

negative control to ensure that false positive $\Delta R_{MQ,ex}$ rates were not detected. To investigate high-molecular weight proteins over 100 K, we performed the methyl-HDR analyses at 4 °C, where the rotational correlation time is estimated to be 65 ns from the intramethyl $^1H-^1H$ dipolar cross-correlation rates.[55]

We prepared a {u-^{2}H, Ileδ1-[$^{13}CH_3$]} MBP sample and acquired a set of methyl-HDR spectra in the presence and absence of the HDR pulses (Figure 2a, Figure S5). The carrier frequency was set on-resonance to Ile132 (^{1}H chemical shift 0.42 ppm, ^{13}C chemical shift 12.5 ppm). The $\Delta R_{MQ,ref}$ and $\Delta R_{MQ,HDR}$ rates were obtained by fitting the intensity ratios as a function of the variable delay, T_{relax} (Figure 2b). Figure 2c shows the plot of the $\Delta R_{MQ,ref}$ and $\Delta R_{MQ,HDR}$ rates of each of the Ileδ1 methyl groups. The average of the $\Delta R_{MQ,HDR}$ rates was 9.3 s^{-1} for the Ileδ1 methyl groups of MBP. This value was consistent with the simulated value of 12.3 s^{-1}, which was calculated from the sum of the $\Delta R_{MQ,DD}$ and $\Delta R_{MQ,CSA}$ rates using the correlation time τ_c = 65 ns, the order parameter S^2 = 0.5 and the atomic coordinates of the crystal structure of MBP (PDB ID: 1DMB).[56] Figure 2d shows the plot of the $\Delta R_{MQ,ex}$ rates calculated using eq 6. The obtained $\Delta R_{MQ,ex}$ rates were smaller than 2.0 s^{-1} for all Ile methyl groups, which is consistent with the absence of significant chemical exchange processes. These results indicate that the $\Delta R_{MQ,ref}$ and $\Delta R_{MQ,HDR}$ rates can be correctly obtained and that false positive $\Delta R_{MQ,ex}$ rates are not detected by the methyl-HDR method. Furthermore, each methyl-HDR spectrum could be obtained within 1 h with a sufficient signal-to-noise ratio despite its large apparent molecular weight, demonstrating the feasibility of the method with high molecular weight proteins.

We also investigated the contributions of the off-resonance effects in the measured $\Delta R_{MQ,HDR}$ rates. We compared the results of two $\Delta R_{MQ,HDR}$ measurements of Ile methyl groups in MBP, one performed under completely on-resonance conditions and the other performed under off-resonance conditions with a single carrier frequency (Figure 2e). The obtained $\Delta R_{MQ,HDR}$ rates from these two measurements were almost identical, and the differences were smaller than 2 s^{-1} in all Ile methyl groups. These results further demonstrate the feasibility of $\Delta R_{MQ,HDR}$ measurements with a single carrier frequency.

Validations of the Methyl-HDR Method in a System with a Chemical Exchange Process. We subsequently applied the method to the HYPA/FBP11 FF domain (molecular mass of 8.2 kDa),[57] which reportedly undergoes a chemical exchange process between the native and folding intermediate states with an exchange rate of around 1800 s^{-1}.[58,59] In addition, its relatively small molecular weight allows the extraction of chemical exchange parameters by established methods. For these reasons, we used the FF domain as a positive control, to test whether or not the accurate $\Delta R_{MQ,ex}$ rates could be measured by the methyl-HDR method.

Before the application of the methyl-HDR method, we performed ^{1}H and ^{13}C single quantum (SQ) CPMG RD analyses to obtain the chemical exchange parameters, k_{ex}, the population of each state and the chemical shift differences, using a {u-^{2}H, Ileδ1-[$^{13}CH_3$], Leu/Val-[$^{13}CH_3$, $^{12}CD_3$]}} FF domain sample.[60,61] The k_{ex} and the population of the folding intermediate state in our sample were 2010 ± 60 s^{-1} and 1.59 ± 0.05%, which agreed well with the reported results of 1880 ± 40 s^{-1} and 1.5 ± 0.4%, respectively.[59]

Then, we applied the methyl-HDR method to the FF domain and obtained the $\Delta R_{MQ,ex}$ rate of each of the Ileδ1, Leu and Val methyl groups. Significantly large $\Delta R_{MQ,ex}$ rates over 10 s^{-1} were detected in some methyl groups, consistent with the results that the FF domain was in the exchange process (Figure 3a). To test that the accurate $\Delta R_{MQ,ex}$ rates were obtained in

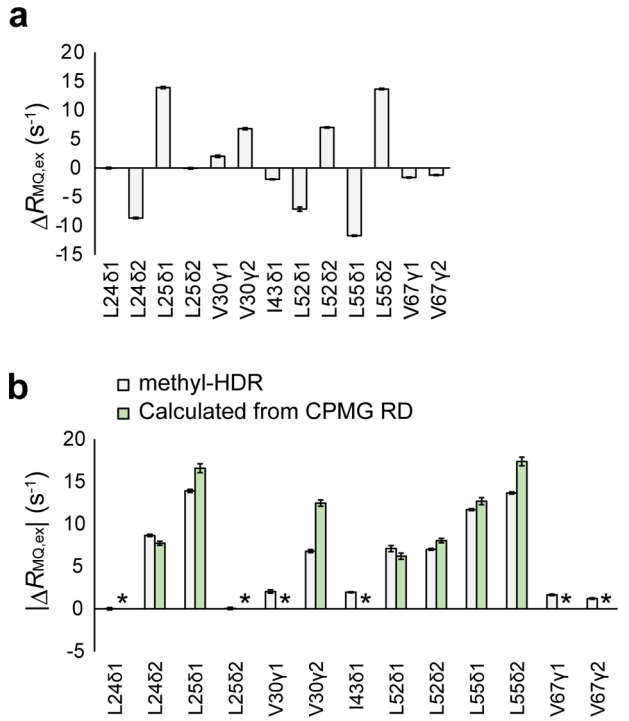

Figure 3. Methyl-HDR results of a {u-^{2}H, Ileδ1-[$^{13}CH_3$], Leu/Val-[$^{13}CH_3$, $^{12}CD_3$]}} FF domain and comparison with the results from the SQ CPMG RD analyses (a) Plot of the $\Delta R_{MQ,ex}$ rates of each Ile, Leu, and Val methyl group in the FF domain. The $\Delta R_{MQ,ex}$ rate of Ile44δ1 is not shown in the plot, because the intensities of s_2 and s_3 in the HDR experiments were too small to be detected and the $\Delta R_{MQ,HDR}$ rate could not be experimentally determined. The measurements were performed at a static magnetic field strength of 14.1 T (600 MHz ^{1}H frequency) using a cryogenic probehead. (b) Plot of the absolute value of the $\Delta R_{MQ,ex}$ rates obtained from the methyl-HDR method (light gray) and that calculated from the CPMG RD experiments (green). Asterisks indicate that the $\Delta R_{MQ,ex}$ rates are expected to be nearly zero from the CPMG RD experiments, due to the small chemical shift differences in either ^{1}H or ^{13}C.

the methyl-HDR analyses, we compared the obtained $\Delta R_{MQ,ex}$ rates with the theoretical $\Delta R_{MQ,ex}$ rates, calculated using the parameters from the SQ CPMG RD analyses and the theoretical equation.[36] (Figure 3b). These two $\Delta R_{MQ,ex}$ rates agreed well with each other (correlation coefficient R = 0.95), indicating that the accurate $\Delta R_{MQ,ex}$ rates were obtained from the methyl-HDR analyses. The validations of the signs of the $\Delta R_{MQ,ex}$ rates are presented in the Supporting Information (Supporting Results 4, Figures S12, S13 and S14). We suppose that the results of the CPMG experiments and the methyl-HDR experiments slightly differ because the two-state chemical exchange assumption does not strictly hold in the FF domain. When we calculate the exchange rates, the populations, and the chemical shift differences, we assume that the exchange process is completely correlated in all methyl groups (i.e., the same k_{ex} and populations), and that only two different states exist in the exchange process. Although this two-state chemical exchange assumption reportedly explains the results of the wild-type FF domain well, mutational analyses suggested that a third unfolded state also exists and is exchanging on the microsecond

DOI: 10.1021/jacs.5b12954
J. Am. Chem. Soc. 2016, 138, 2302−2311

time scale.[58,62,63] Since the CPMG RD experiments and the methyl-HDR methods require the measurements of different NMR parameters and the time scales accessible with the two methods differ, the two methods can give slightly different results when the two-state chemical exchange assumption does not strictly hold. In addition to this, the systematic errors of the two experiments might also lead to the different results. We expect that the systematic errors originated from pulse imperfections, fitting errors,[64] off-resonance effects, small variations in experimental conditions, and so on.

Comparison of the Methyl-HDR Method with the Previously Reported MQ CPMG RD Method. To demonstrate the versatility of the methyl-HDR method, we performed numerical simulations to compare the methyl-HDR method with the MQ CPMG RD method, which was previously reported for analyzing chemical exchange processes based on the methyl-TROSY.[26]

In the MQ CPMG RD method, the exchange contributions can be detected from the deviation of the effective $R_{MQ,eff}$ rates measured in the presence of a ν Hz (typically 50−1000 Hz) CPMG pulse train irradiated on ^{13}C nuclei, $R_{MQ,eff}(\nu)$, where $\nu = 1/(4\tau_{CP})$ and $2\tau_{CP}$ is the spacing between successive 180° pulses. The analytical expression of $R_{MQ,eff}(\nu)$ is described in the original papers.[26,28] We defined the exchanging contributions of the effective R_{MQ} rates, $R_{MQ,ex(CPMG)}$, in eq 7, and investigated their dependence on $\Delta\omega_C$ and $\Delta\omega_H$.

$$R_{MQ,ex(CPMG)} = R_{MQ,eff}(50\ \text{Hz}) - R_{MQ,eff}(1000\ \text{Hz}) \quad (7)$$

The dependence on the $\Delta\omega_C$ and $\Delta\omega_H$ of the $R_{MQ,ex(CPMG)}$ rates calculated with k_{ex} = 3000 s^{-1} and p_B = 5% is shown in Figure 4a and b. The plots show that the $R_{MQ,ex(CPMG)}$ rates significantly increase when the size of $\Delta\omega_C$ is relatively larger than that of $\Delta\omega_H$. However, in the case where significant sizes of both $\Delta\omega_C$ and $\Delta\omega_H$ exist in the chemical exchange processes, the $R_{MQ,ex(CPMG)}$ rates drop to nearly zero or negative values depending on the relative size of $\Delta\omega_H$ to $\Delta\omega_C$, making it difficult to detect and characterize the chemical exchange processes.

In contrast, in the methyl-HDR methods, the exchange contributions can be detected as increases of the $|\Delta R_{MQ,ex}|$ values. Figure 4c and d show the dependence on $\Delta\omega_C$ and $\Delta\omega_H$ of the $\Delta R_{MQ,ex}$ rates calculated under the same conditions as in Figure 4a and b. In contrast to the $R_{MQ,ex(CPMG)}$ rates, the $\Delta R_{MQ,ex}$ rates increase almost linearly with increasing $\Delta\omega_C$ and $\Delta\omega_H$ under these k_{ex} and p_b conditions. Furthermore, the variations of the $\Delta R_{MQ,ex}$ rates tend to be larger than those of the $R_{MQ,ex(CPMG)}$ rates, unless the size of $\Delta\omega_C$ is relatively larger than that of $\Delta\omega_H$. These comparisons demonstrate that the exchange processes that are difficult to characterize by the MQ CPMG RD method can be sensitively detected as the changes in the $\Delta R_{MQ,ex}$ rates.

These considerations obtained from the numerical simulations are demonstrated well in the comparisons of the experimental results of the FF domain. Figure 5a shows the comparison of the experimentally measured $R_{MQ,ex(CPMG)}$ and the $|\Delta R_{MQ,ex}|$ values of the exchanging methyl groups of the FF domain. The $\Delta\omega_C$ and $\Delta\omega_H$ values obtained from the SQ CPMG RD method were also plotted for comparison (Figure 5b and c). The exchange contributions of Leu24δ1 and Leu25δ2, in which only the $\Delta\omega_C$ exists, could be detected as the increased $R_{MQ,ex(CPMG)}$. Similarly, the exchange contributions of the rest of the methyl groups, in which both the $\Delta\omega_C$ and $\Delta\omega_H$ exist, could be more sensitively detected as changes of

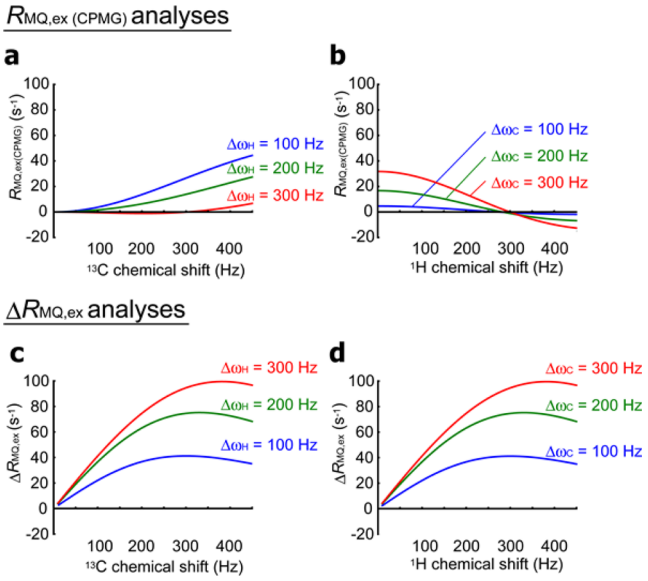

Figure 4. Simulations of the $\Delta R_{MQ,ex}$ rates and the $R_{MQ,ex(CPMG)}$ rates under various ^1H and ^{13}C chemical shift differences. (a) Plots of the $R_{MQ,ex(CPMG)}$ rates versus the ^{13}C chemical shift difference ($\Delta\omega_C$) with three different conditions of ^1H chemical shift differences ($\Delta\omega_H$, 100 Hz in blue, 200 Hz in green, and 300 Hz in red. The same applies to the following plots.). (b) Plots of the $R_{MQ,ex(CPMG)}$ rates versus $\Delta\omega_H$ with three different conditions of $\Delta\omega_C$. (c) Plots of the $\Delta R_{MQ,ex}$ rates versus $\Delta\omega_C$ with three different conditions of $\Delta\omega_H$. (d) Plots of the $\Delta R_{MQ,ex}$ rates versus $\Delta\omega_H$ with three different conditions of $\Delta\omega_C$. The $R_{MQ,ex(CPMG)}$ rates are calculated from the difference of the effective R_{MQ} rates under 50 Hz and 1000 Hz CPMG pulse trains, using the reported analytical expression.[26,28] The $\Delta R_{MQ,ex}$ rates are calculated using the reported analytical expression[36] (eq S7). The exchange rate and minor state population are set to 3000 s^{-1} and 5%.

the $\Delta R_{MQ,ex}$ rates. The most obvious case was Leu52δ1, where the $R_{MQ,ex(CPMG)}$ rate was nearly zero and a flat dispersion profile was obtained (Figure S6). In this methyl group, the existence of the chemical exchange contribution was apparent from the significant increase in the $|\Delta R_{MQ,ex}|$ values. This is due to the large $\Delta\omega_H$ contribution relative to the $\Delta\omega_C$ in Leu52δ1. These results strongly support the conclusion from the numerical simulations and demonstrate the versatility of the methyl-HDR method for characterizing the chemical exchange processes in high molecular weight proteins.

Application: KirBac1.1 Channel with a Molecular Mass over 200 kDa. Since the robustness of the methyl-HDR method was demonstrated by the results obtained with MBP and the FF domain, we applied the method to a more challenging system, KirBac1.1, a prokaryotic inwardly rectifying potassium channel identified in *Burkholderia pseudomallei*,[65,66] which has an apparent molecular mass of over 200 kDa as a functional tetrameric form in detergent micelles.

KirBac1.1 (1−321) was expressed and purified, according to the previous report, with an additional detergent exchange step.[66] The activity of purified KirBac1.1 was confirmed from the accelerated $^{86}Rb^+$ intake of KirBac1.1-reconstituted liposomes relative to the blank liposomes[67] (Figure S7). To alleviate the signal overlapping caused by the increased signal line width, we utilized the HZQC scheme, instead of conventional HMQC, since HZQC achieves line-narrowing effects in the indirect dimension for larger systems, such as KirBac1.1[27,37] (Figure S1). We measured the $^1H-^{13}C$ HZQC spectrum of {u-^2H, Ileδ1-[$^{13}CH_3$]} KirBac1.1 in *n*-dodecyl-β-D-

DOI: 10.1021/jacs.5b12954
J. Am. Chem. Soc. 2016, 138, 2302−2311

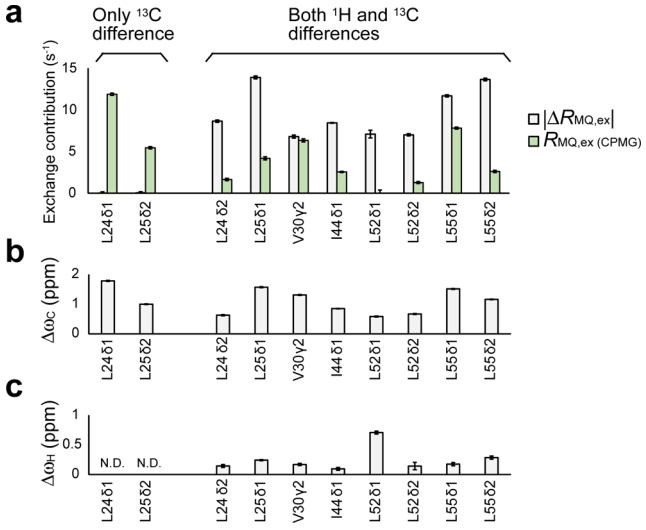

Figure 5. Comparisons of the $\Delta R_{MQ,ex}$ rates and the $R_{MQ,ex(CPMG)}$ rates of exchanging Ile, Leu, and Val methyl groups in FF domain. (a) Comparisons of the absolute values of the $\Delta R_{MQ,ex}$ rates obtained by the methyl-HDR method (gray) and the $R_{MQ,ex(CPMG)}$ rates obtained by the MQ CPMG RD method. (b) Plot of the ^{13}C chemical shift differences obtained from the ^{13}C SQ CPMG RD method. (c) Plot of the ^{1}H chemical shift differences obtained from the ^{1}H SQ CPMG RD method. Methyl groups with only ^{13}C chemical shift differences (Leu24δ1 and Leu25δ2) and those with both ^{1}H and ^{13}C chemical shift differences (Leu24δ2, Leu25δ1, Val30γ2, Ile44δ1, Leu52δ1, Leu52δ2, Leu55δ1, and Leu55δ2) are plotted separately. All of the measurements were performed at a static magnetic field strength of 14.1 T (600 MHz ^{1}H frequency) using a cryogenic probehead.

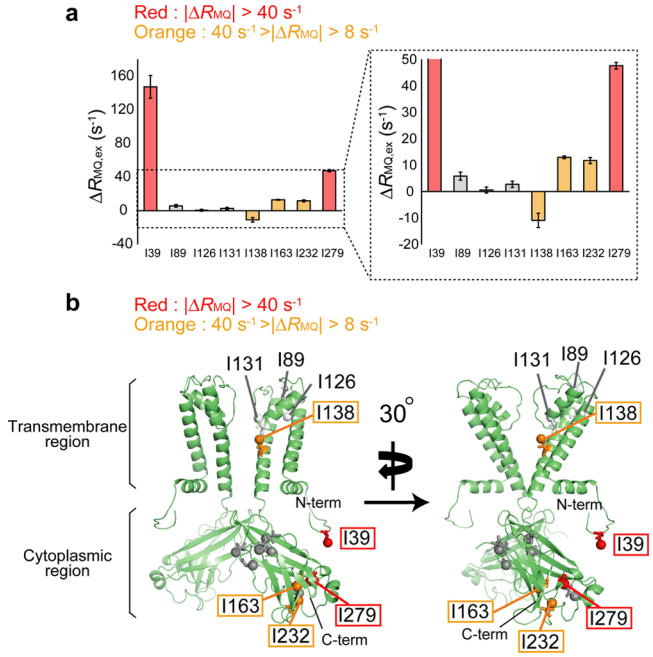

Figure 6. Methyl-HDR results of KirBac1.1. (a) Plot of the $\Delta R_{MQ,ex}$ rates of each Ile methyl group in KirBac1.1. An expanded view of the $\Delta R_{MQ,ex}$ rates from −20 to 50 s^{-1} is also shown. Ile methyl groups with $\Delta R_{MQ,ex}$ rates with absolute values larger than 40 s^{-1} are plotted in red, and those with smaller but significant $\Delta R_{MQ,ex}$ rates with absolute values within the 8.0−40 s^{-1} range are plotted in orange. (b) Mapping of the Ile residues observed with significant $\Delta R_{MQ,ex}$ rates (PDB ID: 1P7B).[66] Only two facing subunits of the tetramer are shown for clarity. The Cδ atoms are shown as spheres in one of the subunits. The Ile methyl groups that were not analyzed are colored black. The Ile methyl groups with significant $\Delta R_{MQ,ex}$ rates are colored in the same manner as in (a).

maltoside (DDM) micelles and assigned 12 methyl signals out of 15 Ile methyl groups, from the comparison of the spectra between the wild type and the mutants in which each Ile was mutated to Val (Figure S8). Three Ile methyl groups (Ile156, Ile257, and Ile298) could not be assigned, due to signal overlapping.

Figure 6a shows the results of methyl-HDR analyses of the Ile methyl groups of KirBac1.1, where the $\Delta R_{MQ,ex}$ rates were successfully obtained from 8 methyl groups. The residues with $\Delta R_{MQ,ex}$ rates with absolute values larger than 40 s^{-1} were Ile39 and Ile279, and those with smaller but significant $\Delta R_{MQ,ex}$ rates with absolute values within the 8.0−40 s^{-1} range were Ile138, Ile163, and Ile232. These methyl groups were located on the N-terminal region (Ile39), the transmembrane helix (Ile138) and the β-strands in the cytoplasmic region (Ile163, Ile232, and Ile279), indicating that significant chemical exchange processes on μs to ms time scales exist in these regions (Figure 6b, Supporting Results 5, Figures S15 and S16). It is worth noting that the chemical exchange processes were observed not only in a transmembrane helix, forming the K^{+}-permeating gate,[66,68] but also in a cytoplasmic region. These results are consistent with the results from crystallographic studies showing the existence of conformational heterogeneity in the cytoplasmic region, which is proposed to be related to the allosteric regulation of the K^{+}-permeating gate in the transmembrane region.[69,70]

DISCUSSION

The Effectiveness of the Methyl-HDR Method. In this research, we developed the methyl-HDR method, which enables the measurements of the chemical exchange contributions in differential MQ relaxation rates, $\Delta R_{MQ,ex}$, of the side-chain methyl groups in high molecular weight proteins. The results from MBP and the HYPA/FBP11 FF domain showed that the accurate $\Delta R_{MQ,ex}$ rates could be obtained by the methyl-HDR method. Moreover, the results from KirBac1.1 showed that the methyl-HDR method could be successfully applied to a larger protein with an apparent molecular mass over 200 kDa.

The methyl-HDR method is not applicable to chemical exchange processes, in which either $\Delta\omega_C$ or $\Delta\omega_H$ is too small to affect the MQ relaxation rates (eq 1) and the extraction of exchange parameters (k_{ex}, p_A, p_B, $\Delta\omega_C$, and $\Delta\omega_H$) is usually difficult solely from the observed $\Delta R_{MQ,ex}$ rates. However, the method is particularly advantageous for studying chemical exchange processes, in which significant chemical shift differences occur in both ^{1}H and ^{13}C nuclei and contribute to the MQ relaxation rate differences. This is in contrast to the previously reported MQ CPMG RD analyses, in which practical applications are often limited to the chemical exchange processes, where only the ^{13}C chemical shift difference contributes to the MQ RD profiles. It was reported that the ^{1}H chemical shifts reflect the surrounding configurations of the aromatic rings,[29] and the ^{13}C chemical shifts reflect the side-chain rotamer distributions.[71−75] It was also reported that, in some cases, the chemical shift changes in ^{1}H are equal to or greater than those in ^{13}C,[76] and provided the valuable structural restraints of the minor conformations.[77] On the basis of these results, the methyl-HDR method, enabling the investigations of

DOI: 10.1021/jacs.5b12954
J. Am. Chem. Soc. 2016, 138, 2302−2311

both the ^{1}H and ^{13}C chemical shift changes, would allow more comprehensive characterizations of the conformational dynamics of proteins, together with the MQ CPMG RD method to investigate the chemical shift changes of ^{13}C.

In the present study, we used the HDR field strength of 10 kHz to effectively suppress the chemical exchange contributions and the off-resonance effects. We suppose that the detailed analysis of the $\Delta R_{MQ,ex}$ dependence on the HDR field strengths would enable the estimation of the exchange rates (eq S15), as originally proposed by Ulzega and co-workers.[43,44] We also note that, in favorable cases, the exchange parameters can be evaluated by simultaneously analyzing the results from both the methyl-HDR and MQ CPMG RD methods, due to the high complementarity of these two methods. When it is difficult to extract chemical exchange parameters solely from the results of the MQ CPMG RD method with high molecular weight proteins, the application of the methyl-HDR method would greatly facilitate the characterization of the chemical exchange processes.

Applications for Investigations of Functional Mechanisms of Proteins. The methyl-HDR method is beneficial for identifying the conformational exchange processes of proteins on μs to ms time scales. There is growing evidence that such conformational exchange processes are closely related to various kinds of protein functions, such as ligand recognition, catalytic reaction, and signal transduction, as evidenced by the strong correlations between the chemical exchange contributions to the transverse relaxation rates (R_{ex}) and their physiological activities.[78−81] Recently, it was reported that the loss of enzymatic activity was linked to changes in μs to ms conformational exchange processes, that were probed by the extensive evaluations of the R_{ex} differences rather than by the differences in crystal structures.[82] Although these R_{ex}-based approaches have only been applicable to smaller proteins so far, the methyl-HDR method would enable similar approaches with high molecular weight proteins, by utilizing the $\Delta R_{MQ,ex}$ rates of the side-chain methyl groups. Therefore, the methyl-HDR method is expected to accelerate the investigations of the relationships between protein dynamics and their functions in high molecular weight proteins, which are difficult to analyze by conventional NMR techniques.

Furthermore, the $\Delta R_{MQ,ex}$ rates measured in the methyl-HDR method are nearly proportional to the product of $\Delta\omega_H$ and $\Delta\omega_C$ in the fast exchange regime (eq 1), making the structural characterizations of the minor conformations feasible. Although care should be taken to ensure that the chemical exchange processes occur in a correlated manner, the size and sign of the $\Delta R_{MQ,ex}$ rates can be utilized to elucidate the structural properties of the minor conformation, by analyzing the correlation between the $\Delta R_{MQ,ex}$ rates and the patterns of chemical shift changes induced by ligand binding, protein modification, mutation and so on.[83,84] The structural characterizations of the minor conformations would greatly clarify the mechanisms by which they are related to the functions.

In this research, we performed the methyl-HDR analyses with the side chain methyl groups from the Ileδ1, Leuδ and Valγ positions. The method can also be applied, in principle, to other methyl groups from the Alaβ,[85] Metε,[86] Ileγ2,[87] and Thrγ2[88] positions, enabling more comprehensive structural and dynamic analyses of proteins. Furthermore, methyl $^{1}H-^{13}C$ labeling strategies in deuterated backgrounds have recently been established in yeast[89,90] and insect cell/baculovirus expression systems,[91] as well as *E. coli* expression systems,[46] which will further extend the applications of the method.

CONCLUSIONS

In summary, we have presented the methyl-HDR method for quantifying chemical exchanges on μs to ms time scales by utilizing the differential multiple quantum relaxation in high molecular weight proteins. The robustness of the method was validated from the results obtained with MBP and the FF domain. We applied the established method to KirBac1.1, with a molecular mass of over 200 kDa, and identified the regions that exist in a chemical exchange process. Applications of the methyl-HDR method, along with the MQ CPMG RD method, will enable the further elucidations of the functional dynamics of biologically important systems, such as membrane proteins and functional protein complexes, which have been difficult to analyze by conventional NMR methods due to molecular size limitations.

ASSOCIATED CONTENT

Supporting Information

The Supporting Information is available free of charge on the ACS Publications website at DOI: 10.1021/jacs.5b12954.

Simulations of $\Delta R_{MQ,ex}$ rates under HDR conditions, experimental evaluations of off-resonance effects in methyl-HDR experiments, consideration of the methyl-TROSY components during HDR, the signs of chemical shift differences in the FF domain, evaluations of line widths of Ile methyl signals of KirBac1.1, detailed experimental procedures, the HZQC version of the methyl-HDR experiment, methyl-HDR spectra of MBP under HDR conditions, MQ CPMG RD analyses of FF domain, functional assay of KirBac1.1, HZQC spectrum of KirBac1.1. (PDF)

AUTHOR INFORMATION

Corresponding Author

*shimada@iw-nmr.f.u-tokyo.ac.jp

Present Address

§Keio University Faculty of Pharmacy, Division of Physics for Life Functions, 1-5-30 Shibakoen, Minato-ku, 105-8512, Japan.

Notes

The authors declare no competing financial interest.

ACKNOWLEDGMENTS

$^{86}Rb^{+}$ intake assays of KirBac1.1 were performed with the support of the Radioisotope Center, The University of Tokyo. This work was supported in part by grants from the Ministry of Economy, Trade, and Industry (METI) (Grant name: Development of core technologies for innovative drug development based upon IT, to I.S.), and a Grant-in-Aid for Scientific Research on Priority Areas from the Japanese Ministry of Education, Culture, Sports, Science, and Technology (to M.O. and I.S.).

REFERENCES

(1) Baldwin, A. J.; Kay, L. E. *Nat. Chem. Biol.* **2009**, *5*, 808−814.

(2) Osawa, M.; Takeuchi, K.; Ueda, T.; Nishida, N.; Shimada, I. *Curr. Opin. Struct. Biol.* **2012**, *22*, 660−669.

(3) Palmer, A. G.; Kroenke, C. D.; Loria, J. P. *Methods Enzymol.* **2001**, *339*, 204−238.

DOI: 10.1021/jacs.5b12954
J. Am. Chem. Soc. 2016, 138, 2302−2311

(4) Eaton, W. A.; Munoz, V.; Hagen, S. J.; Jas, G. S.; Lapidus, L. J.; Henry, E. R.; Hofrichter, J. *Annu. Rev. Biophys. Biomol. Struct.* **2000**, *29*, 327−359.
(5) Hammes, G. G. *Biochemistry* **2002**, *41*, 8221−8228.
(6) Montelione, G. T.; Wagner, G. *J. Am. Chem. Soc.* **1989**, *111*, 3096−3098.
(7) Farrow, N. A.; Zhang, O. W.; Formankay, J. D.; Kay, L. E. *J. Biomol. NMR* **1994**, *4*, 727−734.
(8) Vallurupalli, P.; Bouvignies, G.; Kay, L. E. *J. Am. Chem. Soc.* **2012**, *134*, 8148−8161.
(9) Carver, J. P.; Richards, R. E. *J. Magn. Reson.* **1972**, *6*, 89−105.
(10) Davis, D. G.; Perlman, M. E.; London, R. E. *J. Magn. Reson., Ser. B* **1994**, *104*, 266−275.
(11) Kroenke, C. D.; Loria, J. P.; Lee, L. K.; Rance, M.; Palmer, A. G. *J. Am. Chem. Soc.* **1998**, *120*, 7905−7915.
(12) Szyperski, T.; Luginbuhl, P.; Otting, G.; Guntert, P.; Wuthrich, K. *J. Biomol. NMR* **1993**, *3*, 151−164.
(13) Mulder, F. A. A.; Mittermaier, A.; Hon, B.; Dahlquist, F. W.; Kay, L. E. *Nat. Struct. Biol.* **2001**, *8*, 932−935.
(14) Boehr, D. D.; McElheny, D.; Dyson, H. J.; Wright, P. E. *Proc. Natl. Acad. Sci. U. S. A.* **2010**, *107*, 1373−1378.
(15) Whittier, S. K.; Hengge, A. C.; Loria, J. P. *Science* **2013**, *341*, 899−903.
(16) Korzhnev, D. M.; Salvatella, X.; Vendruscolo, M.; Di Nardo, A. A.; Davidson, A. R.; Dobson, C. M.; Kay, L. E. *Nature* **2004**, *430*, 586−590.
(17) Morrison, E. A.; DeKoster, G. T.; Dutta, S.; Vafabakhsh, R.; Clarkson, M. W.; Bahl, A.; Kern, D.; Ha, T.; Henzler-Wildman, K. A. *Nature* **2012**, *481*, 45−U50.
(18) Palmer, A. G.; Grey, M. J.; Wang, C. Y. *Methods Enzymol.* **2005**, *394*, 430−465.
(19) Cavanagh, J.; Fairbrother, W. J.; Palmer, A. G.; Rance, M.; Skelton, N. J. *Protein NMR Spectroscopy: Principles and Practice*, 2nd ed.; Elsevier Academic Press: San Diego, 2007.
(20) Tugarinov, V.; Hwang, P. M.; Ollerenshaw, J. E.; Kay, L. E. *J. Am. Chem. Soc.* **2003**, *125*, 10420−10428.
(21) Ollerenshaw, J. E.; Tugarinov, V.; Kay, L. E. *Magn. Reson. Chem.* **2003**, *41*, 843−852.
(22) Sprangers, R.; Gribun, A.; Hwang, P. M.; Houry, W. A.; Kay, L. E. *Proc. Natl. Acad. Sci. U. S. A.* **2005**, *102*, 16678−16683.
(23) Sprangers, R.; Kay, L. E. *Nature* **2007**, *445*, 618−622.
(24) Religa, T. L.; Sprangers, R.; Kay, L. E. *Science* **2010**, *328*, 98−102.
(25) Rosenzweig, R.; Kay, L. E. *Annu. Rev. Biochem.* **2014**, *83*, 291−315.
(26) Korzhnev, D. M.; Kloiber, K.; Kanelis, V.; Tugarinov, V.; Kay, L. E. *J. Am. Chem. Soc.* **2004**, *126*, 3964−3973.
(27) Gill, M. L.; Palmer, A. G. *J. Biomol. NMR* **2011**, *51*, 245−251.
(28) Korzhnev, D. M.; Kloiber, K.; Kay, L. E. *J. Am. Chem. Soc.* **2004**, *126*, 7320−7329.
(29) Perkins, S. J.; Wuthrich, K. *Biochim. Biophys. Acta, Protein Struct.* **1979**, *576*, 409−423.
(30) Fruh, D.; Tolman, J. R.; Bodenhausen, G.; Zwahlen, C. *J. Am. Chem. Soc.* **2001**, *123*, 4810−4816.
(31) Tessari, M.; Vuister, G. W. *J. Biomol. NMR* **2000**, *16*, 171−174.
(32) Kloiber, K.; Konrat, R. *J. Biomol. NMR* **2000**, *18*, 33−42.
(33) Reif, B.; Hennig, M.; Griesinger, C. *Science* **1997**, *276*, 1230−1233.
(34) Chiarparin, E.; Pelupessy, P.; Ghose, R.; Bodenhausen, G. *J. Am. Chem. Soc.* **1999**, *121*, 6876−6883.
(35) Pellecchia, M.; Pang, Y. X.; Wang, L. C.; Kurochkin, A. V.; Kumar, A.; Zuiderwegt, E. R. P. *J. Am. Chem. Soc.* **1999**, *121*, 9165−9170.
(36) Wang, C. Y.; Palmer, A. G. *J. Biomol. NMR* **2002**, *24*, 263−268.
(37) Tugarinov, V.; Sprangers, R.; Kay, L. E. *J. Am. Chem. Soc.* **2004**, *126*, 4921−4925.
(38) Ergel, B.; Gill, M. L.; Brown, L.; Yu, B. M.; Palmer, A. G.; Hunt, J. F. *J. Biol. Chem.* **2014**, *289*, 29584−29601.
(39) Tugarinov, V.; Scheurer, C.; Bruschweiler, R.; Kay, L. E. *J. Biomol. NMR* **2004**, *30*, 397−406.
(40) Konrat, R.; Sterk, H. *Chem. Phys. Lett.* **1993**, *203*, 75−80.
(41) Norwood, T. J.; Tillett, M. L.; Lian, L. Y. *Chem. Phys. Lett.* **1999**, *300*, 429−434.
(42) Verde, M.; Ulzega, S.; Ferrage, F.; Bodenhausen, G. *J. Chem. Phys.* **2009**, *130*, 130.
(43) Ulzega, S.; Salvi, N.; Segawa, T. F.; Ferrage, F.; Bodenhausen, G. *ChemPhysChem* **2011**, *12*, 333−341.
(44) Salvi, N.; Ulzega, S.; Ferrage, F.; Bodenhausen, G. *J. Am. Chem. Soc.* **2012**, *134*, 2481−2484.
(45) Ulzega, S.; Verde, M.; Ferrage, F.; Bodenhausen, G. *J. Chem. Phys.* **2009**, *131*, 224503.
(46) Goto, N. K.; Gardner, K. H.; Mueller, G. A.; Willis, R. C.; Kay, L. E. *J. Biomol. NMR* **1999**, *13*, 369−374.
(47) Shaka, A. J.; Keeler, J.; Frenkiel, T.; Freeman, R. *J. Magn. Reson.* **1983**, *52*, 335−338.
(48) Wang, A. C.; Bax, A. *J. Biomol. NMR* **1993**, *3*, 715−720.
(49) Marion, D.; Ikura, M.; Tschudin, R.; Bax, A. *J. Magn. Reson.* **1989**, *85*, 393−399.
(50) Pelupessy, P.; Ferrage, F.; Bodenhausen, G. *J. Chem. Phys.* **2007**, *126*, 126.
(51) Allard, P.; Helgstrand, M.; Hard, T. *J. Magn. Reson.* **1998**, *134*, 7−16.
(52) Ban, D.; Gossert, A. D.; Giller, K.; Becker, S.; Griesinger, C.; Lee, D. *J. Magn. Reson.* **2012**, *221*, 1−4.
(53) Kovacs, H.; Gossert, A. *J. Biomol. NMR* **2014**, *58*, 101−112.
(54) Gardner, K. H.; Zhang, X. C.; Gehring, K.; Kay, L. E. *J. Am. Chem. Soc.* **1998**, *120*, 11738−11748.
(55) Sun, H. C.; Kay, L. E.; Tugarinov, V. *J. Phys. Chem. B* **2011**, *115*, 14878−14884.
(56) Sharff, A. J.; Rodseth, L. E.; Quiocho, F. A. *Biochemistry* **1993**, *32*, 10553−10559.
(57) Allen, M.; Friedler, A.; Schon, O.; Bycroft, M. *J. Mol. Biol.* **2002**, *323*, 411−416.
(58) Korzhnev, D. M.; Religa, T. L.; Banachewicz, W.; Fersht, A. R.; Kay, L. E. *Science* **2010**, *329*, 1312−1316.
(59) Latham, M. P.; Kay, L. E. *J. Mol. Biol.* **2014**, *426*, 3214−3220.
(60) Lundstrom, P.; Vallurupalli, P.; Religa, T. L.; Dahlquist, F. W.; Kay, L. E. *J. Biomol. NMR* **2007**, *38*, 79−88.
(61) Tugarinov, V.; Kay, L. E. *J. Am. Chem. Soc.* **2007**, *129*, 9514−9521.
(62) Jemth, P.; Gianni, S.; Day, R.; Li, B.; Johnson, C. M.; Daggett, V.; Fersht, A. R. *Proc. Natl. Acad. Sci. U. S. A.* **2004**, *101*, 6450−6455.
(63) Korzhnev, D. M.; Religa, T. L.; Lundstrom, P.; Fersht, A. R.; Kay, L. E. *J. Mol. Biol.* **2007**, *372*, 497−512.
(64) Ishima, R.; Torchia, D. A. *J. Biomol. NMR* **2005**, *32*, 41−54.
(65) Durell, S. R.; Guy, H. R. *BMC Evol. Biol.* **2001**, *1*, 14.
(66) Kuo, A. L.; Gulbis, J. M.; Antcliff, J. F.; Rahman, T.; Lowe, E. D.; Zimmer, J.; Cuthbertson, J.; Ashcroft, F. M.; Ezaki, T.; Doyle, D. A. *Science* **2003**, *300*, 1922−1926.
(67) Enkvetchakul, D.; Bhattacharyya, J.; Jeliazkova, I.; Groesbeck, D. K.; Cukras, C. A.; Nichols, C. G. *J. Biol. Chem.* **2004**, *279*, 47076−47080.
(68) Bavro, V. N.; De Zorzi, R.; Schmidt, M. R.; Muniz, J. R. C.; Zubcevic, L.; Sansom, M. S. P.; Venien-Bryan, C.; Tucker, S. J. *Nat. Struct. Mol. Biol.* **2012**, *19*, 158−163.
(69) Yokogawa, M.; Osawa, M.; Takeuchi, K.; Mase, Y.; Shimada, I. *J. Biol. Chem.* **2011**, *286*, 2215−2223.
(70) Whorton, M. R.; MacKinnon, R. *Nature* **2013**, *498*, 190−197.
(71) London, R. E.; Wingad, B. D.; Mueller, G. A. *J. Am. Chem. Soc.* **2008**, *130*, 11097−11105.
(72) Mulder, F. A. A. *ChemBioChem* **2009**, *10*, 1477−1479.
(73) Butterfoss, G. L.; DeRose, E. F.; Gabel, S. A.; Perera, L.; Krahn, J. M.; Mueller, G. A.; Zheng, X. H.; London, R. E. *J. Biomol. NMR* **2010**, *48*, 31−47.
(74) Hansen, D. F.; Neudecker, P.; Vallurupalli, P.; Mulder, F. A. A.; Kay, L. E. *J. Am. Chem. Soc.* **2010**, *132*, 42−43.

DOI: 10.1021/jacs.5b12954
J. Am. Chem. Soc. 2016, 138, 2302−2311

(75) Hansen, D. F.; Kay, L. E. *J. Am. Chem. Soc.* **2011**, *133*, 8272−8281.
(76) Weininger, U.; Liu, Z. H.; McIntyre, D. D.; Vogel, H. J.; Akke, M. *J. Am. Chem. Soc.* **2012**, *134*, 18562−18565.
(77) Hansen, A. L.; Lundstrom, P.; Velyvis, A.; Kay, L. E. *J. Am. Chem. Soc.* **2012**, *134*, 3178−3189.
(78) Volkman, B. F.; Lipson, D.; Wemmer, D. E.; Kern, D. *Science* **2001**, *291*, 2429−2433.
(79) Eisenmesser, E. Z.; Bosco, D. A.; Akke, M.; Kern, D. *Science* **2002**, *295*, 1520−1523.
(80) Kalodimos, C. G.; Biris, N.; Bonvin, A. M. J. J.; Levandoski, M. M.; Guennuegues, M.; Boelens, R.; Kaptein, R. *Science* **2004**, *305*, 386−389.
(81) Villinger, S.; Briones, R.; Giller, K.; Zachariae, U.; Lange, A.; de Groot, B. L.; Griesinger, C.; Becker, S.; Zweckstetter, M. *Proc. Natl. Acad. Sci. U. S. A.* **2010**, *107*, 22546−22551.
(82) Bhabha, G.; Lee, J.; Ekiert, D. C.; Gam, J.; Wilson, I. A.; Dyson, H. J.; Benkovic, S. J.; Wright, P. E. *Science* **2011**, *332*, 234−238.
(83) Massi, F.; Wang, C. Y.; Palmer, A. G. *Biochemistry* **2006**, *45*, 10787−10794.
(84) Masterson, L. R.; Cheng, C.; Yu, T.; Tonelli, M.; Kornev, A.; Taylor, S. S.; Veglia, G. *Nat. Chem. Biol.* **2010**, *6*, 821−828.
(85) Isaacson, R. L.; Simpson, P. J.; Liu, M.; Cota, E.; Zhang, X.; Freemont, P.; Matthews, S. *J. Am. Chem. Soc.* **2007**, *129*, 15428−15429.
(86) Fischer, M.; Kloiber, K.; Hausler, J.; Ledolter, K.; Konrat, R.; Schmid, W. *ChemBioChem* **2007**, *8*, 610−612.
(87) Ruschak, A. M.; Velyvis, A.; Kay, L. E. *J. Biomol. NMR* **2010**, *48*, 129−135.
(88) Velyvis, A.; Ruschak, A. M.; Kay, L. E. *PLoS One* **2012**, *7*, e43725.
(89) Miyazawa-Onami, M.; Takeuchi, K.; Takano, T.; Sugiki, T.; Shimada, I.; Takahashi, H. *J. Biomol. NMR* **2013**, *57*, 297−304.
(90) Clark, L.; Zahm, J. A.; Ali, R.; Kukula, M.; Bian, L. Q.; Patrie, S. M.; Gardner, K. H.; Rosen, M. K.; Rosenbaum, D. M. *J. Biomol. NMR* **2015**, *62*, 239−245.
(91) Kofuku, Y.; Ueda, T.; Okude, J.; Shiraishi, Y.; Kondo, K.; Mizumura, T.; Suzuki, S.; Shimada, I. *Angew. Chem., Int. Ed.* **2014**, *53*, 13376−13379.

DOI: 10.1021/jacs.5b12954
J. Am. Chem. Soc. 2016, 138, 2302−2311